

INTERANNUAL VARIABILITY OF THE NORTHWESTWARD PROPAGATION OF COLD AIR SURGES ACROSS THE ROSS ICE SHELF

Jorge F. Carrasco*
 Dirección Meteorológica de Chile and
 Centro de Estudios Científicos

David H. Bromwich
 Polar Meteorology Group
 Byrd Polar Research Center
 The Ohio State University
 Columbus, Ohio – USA

1. INTRODUCTION

Numerical model simulation of the katabatic wind regime in the Antarctic continent (e.g. Parish and Bromwich 1987, 1991) shows that the airflow descending from the high plateau of East and West Antarctica converges toward several coastal zones. In particular in the Ross Ice Shelf (RIS) region, a large convergence zone takes place at the Siple Coast and some of the major glaciers that dissect the Transantarctic Mountains (Figure 1). On the other hand, cloud-free infrared satellite images occasionally reveal dark signatures extending from the bottom of the glaciers and Siple Coast toward the north and northwest on the

RIS. The location and orientation of these dark signatures suggest that they are associated with the cold katabatic winds descending from the plateau; vertical mixing associated with katabatic winds causes the near surface temperature to rise while the boundary layer as a whole remains cooler than the surroundings. One of the prominent features is the dark signature that extends almost parallel to the Transantarctic Mountain, which is associated with the katabatic airflow that descends from the Marie Byrd Land and intermittently propagates northwestward toward the Ross Sea. Previous studies (Bromwich et al.

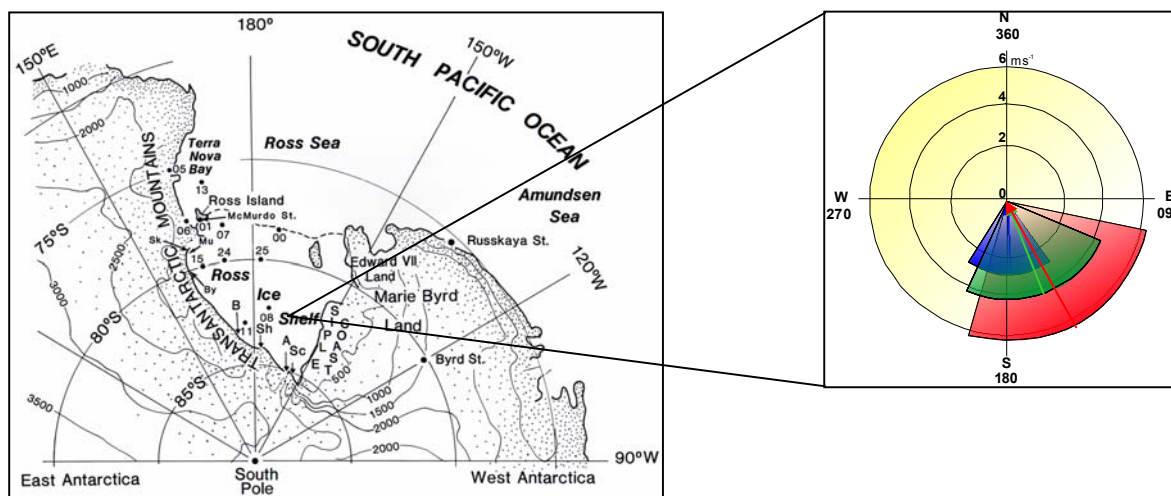


Figure 1. Location map. Number 08 identifies location of AWS Lettau. Wind speed and direction at Lettau is indicated. Color solid lines across the concentric circles are the mean direction and its length indicates the magnitude for: all days (green), only colder days (blue) and only KW_days (red). The triangle encloses ± 1 s.d. of the wind direction.

1992, 1993) for April-August 1988, revealed that when these katabatic events took place the automatic weather stations (AWS) in the southern

part of the RIS, in particular the AWS Lettau (Figure 1), registered increases in the near surface air temperature, in the pressure gradient normal to the Transantarctic Mountains, in the wind speed, and a more southeasterly wind direction (Figure 1). These findings (mainly the air temperature) were examined over the 1986 – 2004 period to study the interannual behavior of

* Corresponding author address: Jorge F. Carrasco, Dirección Meteorológica de Chile, Av. Portales 3450, Santiago, Chile, email: jorge.carrasco@meteochile.cl

the katabatic wind events that take place during the winter months April to August.

2. PROCEDURE AND DEFINITIONS

AWS Lettau (number 08 in the map) is located in the path of the katabatic airflow that propagates toward the northwest across the RIS. When this happens, AWSs Elaine (11) and Gill (25) also capture the katabatic winds blowing northwestward. Data analysis of concurrent observations for 1988 revealed a correlation of 0.78 (0.81) and 0.73 (0.75) between Lettau and Elaine (Lettau and Gill) for the daily average and the three-hourly air temperature observations, respectively. These correlations support the procedure of filling the gaps of missing data at Lettau station using observations from Gill and/or Elaine. Thus, a complete data series for winter was constructed for the 1986-2004 period. The annual seasonal behavior of the air temperature was obtained by applying the exponential filter (Equations 1 and 2) through the daily average data to the April-August period (see Rosenblüth et al 1997). This is:

$$y_t = cx_t + (1 - c)y_{t-1}, \quad t = 2, 3, \dots, n \quad (1)$$

For the first forward smoothing and,

$$z_t = cy_t + (1 - c)z_{t-1} \quad (2)$$

$$t = (n - 1), (n - 2), \dots, 1$$

For the second backward smoothing in time

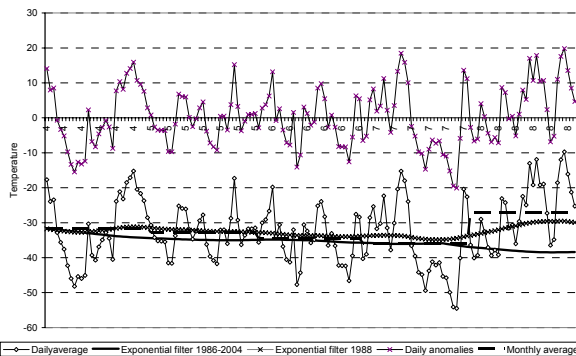


Figure 2. Temperature behavior at AWS Lettau during 1988. Thick black is the exponential filter applied to the 1986-2004 daily average. Grey line-cross is the exponential average applied to the daily mean for 1988. Dashed thick lines are the individual monthly means for 1988. Thin line with squares (at the bottom) is the daily average while the thin line with crosses (at the top) shows the daily anomalies.

where c was arbitrarily taken as 0.05 in order to filter out the daily and synoptic scale variability.

This gives a smooth seasonal mean that overcomes the jumps that are produced when the individual monthly averages are used (see Figure 2). This procedure was applied for each year from 1986 to 2004. Then the daily anomalies were calculated with respect to each seasonal mean, where a warm day (w_day) was defined as all those days when the surface air temperature, at the bottom of the RIS as measured by AWS Lettau, was 1 s.d. above the respective daily seasonal average given by the exponential filter in each year. Likewise, non- w_days (or cold_days) are those days when the air surface temperature at AWS Lettau was 1 s.d. colder than the respective daily average given by the exponential filter. As with previous studies, a katabatic warm event (KWE) and non-katabatic cold event (non-KWE) were respectively defined to occur when at least two consecutive w_days and two non- w_days took place. Even though, the wind speed and wind direction can also be a good indicator for detecting the occurrence of katabatic wind events (Figure 1), it is not used because of the large gaps with missing data.

3. RESULTS

3.1 Interannual behavior of the KWE

The winter average of total w_days was 57.0 ± 5.8 days (1 s.d.) and total KWE was 12.6 ± 2.1 episodes for 1986-2004 (Table 1). About 51.9 ± 5.9 w_days per year were associated with KWE, which means that 5.1 ± 2.8 days counted as events of less than 2-days duration. This means that about 91% of the w_days can be categorized as katabatic warm days (kw_days). The annual behavior can graphically be seen in Figure 3. The correlation between w_days and kw_days is 0.89 (statistically significant at 1% level), and between w_days and KWE as well as between kw_days and KWE is 0.54 (statistically significant at 5% level in both cases). Despite the interannual variability, an overall decrease of the katabatic events (and katabatic days) is revealed by the negative linear trend during the 1986-2004 period, while at the same time, an increase in the non-katabatic wind events, or number of colder days, is shown by the analysis. In fact, a cooling of -0.11 °C per year is found by the linear trend applied to the winter average for the period ((statistically significant at 5% level), also see Figure 2 in Doran et al. 2002).

An analysis of the ice concentration offshore of the northwestern edge of the RIS (just

Table 1. Winter-average of total warmer (w_days) and colder days ($non-w_days$) and katabatic wind event (KWE) and duration as measured by the air temperature registered at the bottom of the RIS.

Year	KW_days	Non-KW_days	KWE	Duration
1986	64	50	14	4.1
1987	55	57	14	3.8
1988	58	60	15	3.8
1989	58	63	10	5.2
1990	63	58	14	4.3
1991	58	66	10	5.0
1992	47	65	13	3.2
1993	57	64	14	4.2
1994	66	56	15	4.3
1995	63	65	15	4.2
1996	61	50	16	3.7
1997	51	64	11	3.9
1998	53	60	13	3.7
1999	47	72	9	5.0
2000	59	60	12	4.4
2001	65	61	12	4.9
2002	50	77	10	5.1
2003	54	59	13	3.9
2004	54	66	10	5.2
Mean	57±5.8	61.7±6.5	12.6±2.1	4.3

east of the Ross Island) was conducted for August, which corresponds to the end month of our winter period. For this, the data were obtained from the National Centers for Environmental Prediction, (NCEP) through its internet page (nomad2.ncep.noaa.gov). The data were displayed on the computer screen and the average ice concentration was evaluated for the region immediately offshore of the RIS up to latitude 77°S and between 170°E to 170°W.

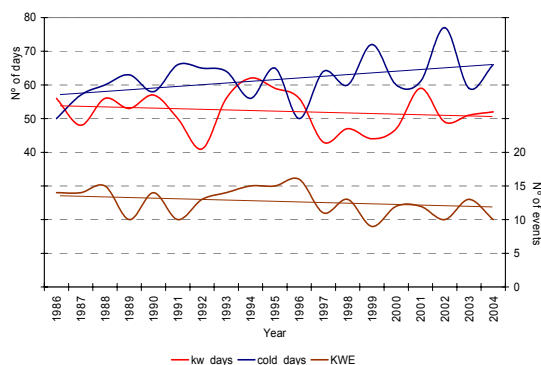


Figure 3. Interannual behavior of the seasonal (April – August) katabatic wind days (red curve: kw_day) and non-katabatic wind days or cold days (blue curve: $cold_days$). Also included is the number of katabatic warm events (brown curve: KWE). Only linear trends for $cold_days$ and KWE are statistically significant at 5% level.

Figure 4 shows the annual number of KWE along with the average ice concentration in August. In general, years with maximum (minimum) ice concentration coincide with years of lower (higher) KWE. The correlation between both is -0.52 for the whole period, which increases to -0.63 for the 1986-2002 period (statistically significant at 5% level in both cases). Also, the linear trend reveals an increase ice concentration offshore the RIS. This out of phase behavior indicates the influence of the katabatic airflow upon the sea ice formation and spring-summer northward extension of the sea-ice disintegration in the Ross Sea region (Bromwich 1992, Bromwich et al. 1998, Jacobs and Comiso 1989).

3.2 Southern atmospheric circulation and KWE

Large-scale anomaly compose analyses were constructed using the NCEP/NCAR Reanalysis and were directly obtained from the webpage of the Climate Diagnosis Center (CDC, www.cdc.noaa.gov). The dates for peak warm days of each KWE were compiled and used to obtain the composite maps for 925 hPa (near surface analysis), 500 hPa (midtropospheric analysis), and 1000-500 hPa thickness (midtropospheric temperature analysis).

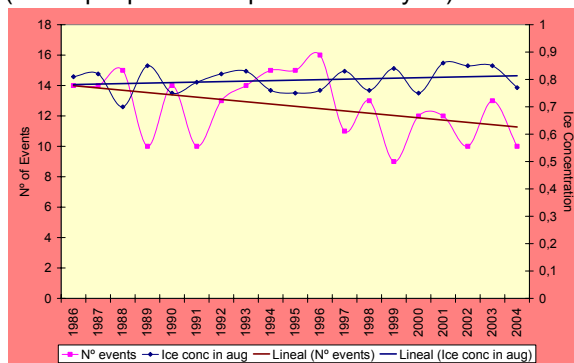


Figure 4. Interannual behavior of the KWE and the ice concentration for August. The slope of the linear trend for the ice concentration is not statistically significant, while for KWE it is statistically significant at 10% level.

The same was done for peak of non-KWE. Figure 5 shows anomalies for non-KWE and KWE at 925 hPa and 500 hPa. Negative anomalies prevail in Antarctica for non-KWE at the 925-hPa level, mainly in the southern Antarctic Peninsula. Positive anomalies occur between 40 and 55 °S, approximately, mainly centered in the Atlantic and Indian oceans and in the western Pacific Ocean.

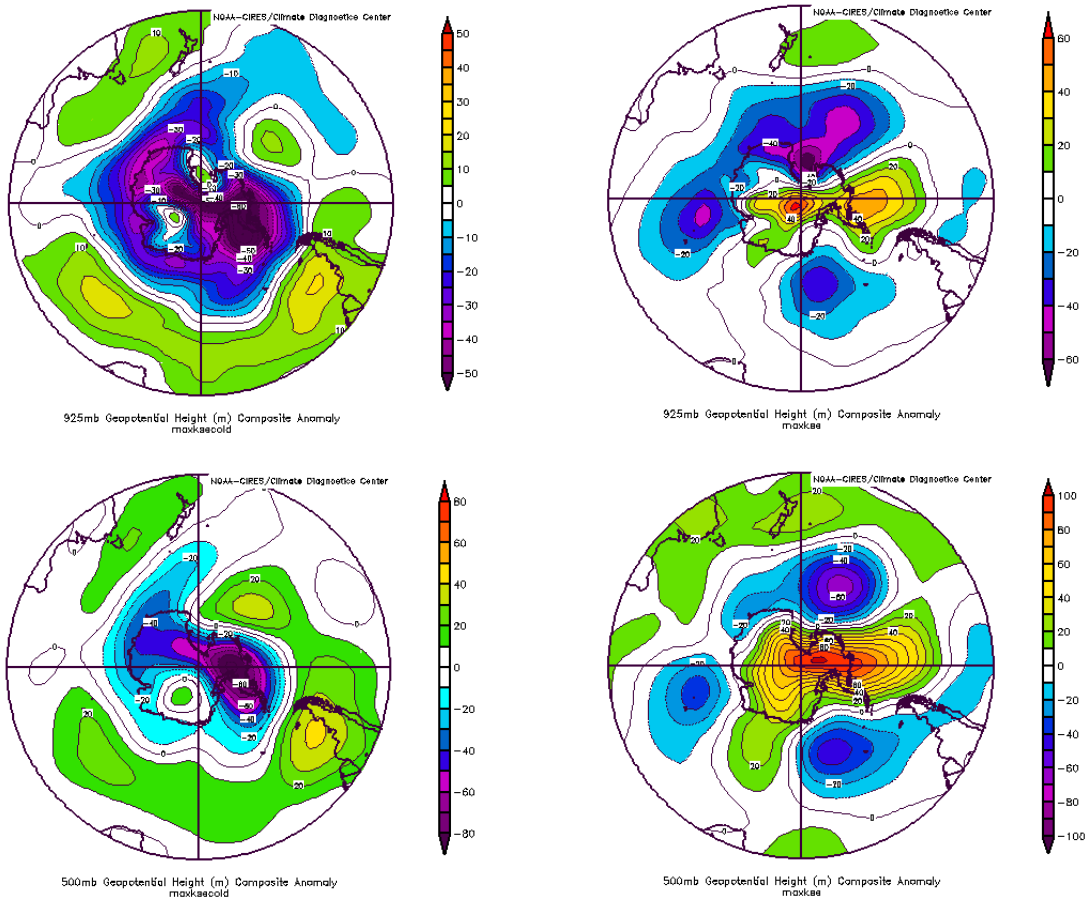


Figure 5. Anomalies of the 925 hPa (top) and 500 hPa (bottom) for peak of non_KWE (left panels) and KWE (right panels).

At 500 hPa, the negative anomalies are more confined to the Antarctic continent, centered in the southern Antarctic Peninsula and extending toward East Antarctica. This picture almost reverses for KWE in both 925 and 500 hPa anomaly composites, where now the positive anomalies dominate the Antarctic Peninsula region with the maximum centered in the Bellingshausen Sea area and near the South Pole. Centers of negative anomalies are located in the southern Pacific, Atlantic and Indian oceans, just north of the Antarctic continent (northeast of Ross Sea, north of Amery Ice Shelf and north of Queen Maud Land). At 925 hPa, the larger negative anomaly is located just to the northeast of the Ross Sea. The anomaly pattern at 500 hPa for peak-KWE shows a wave number 3 while for non-KWE it shows a wave number 1-2. The anomaly patterns described above indicate that for non-KWE that the Antarctic anticyclone

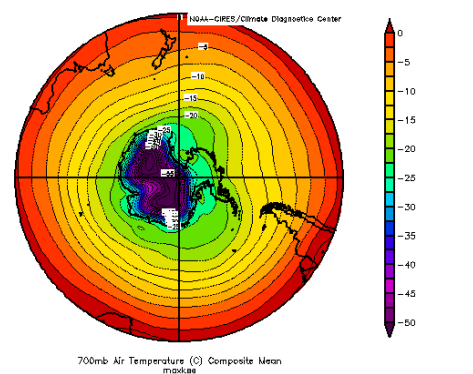


Figure 6. Composite of 1000-500 hPa geopotential thickness for KWE.

and the cyclonic activity in the “westerly band” are weaker than the average. On the other hand, for KWE the near surface hemispheric pattern reveals a stronger Antarctic anticyclone and more

cyclonic activity surrounding the continent (intensified circumpolar trough), mainly near the Ross Sea. This pattern is similar to the one found by Bromwich et al. (1993) for the 1988 study. Under this situation, synoptic-scale cyclones near Ross Sea increase the pressure gradient perpendicular to the Transantarctic Mountains and support the northwestward propagation of the katabatic airflow. The cold characteristic of the descending air is revealed by the 1000-500 hPa thickness analysis (Figure 6) which shows a cold trough over the RIS and Ross Sea region.

4. DISCUSSION

An immediate effect of the katabatic airflow is observed in the ice concentration offshore from the RIS (cor: -0.52). A decreased ice concentration in winters with more katabatic events reveals that more open water/thin ice areas (polynyas) occur within the ice pack offshore from the RIS. Zwally et al. (1985) indicated that the permanent polynya just to the east of Ross Island fluctuates in size according to the synoptic-scale support. Bromwich et al. (1992, 1993, 1998) later confirmed this by showing that the synoptic-scale pattern supports the northwestward propagation of the katabatic airflow across the RIS. Therefore, relatively cold air blowing off the edge of the RIS interacts with the sea ice and open water, playing a role in the formation and enlargement of the coastal polynya. The main feature of large-scale composite analyses for KWE is the negative height anomalies just to the north of the Ross Sea, along with positive height anomalies centered to the west of the Antarctic Peninsula and near the South Pole. These anomalies indicate that for KWE there is a synoptic-scale cyclonic circulation supporting the airflow moving parallel to the Transantarctic Mountains. The anomaly composite for non-KWE analysis resembles the first principal component (PC) mode (or Empirical Orthogonal Function, EOF 1; Thompson and Wallace 2000, Codron 2005), which captures the variability of the atmospheric circulation in the Southern Hemisphere extratropics and is known as the Antarctic Oscillation (AAO) or the Southern Hemisphere Annular Mode (SAM). In its positive phase, the SAM suggests a stronger polar vortex (Thompson and Solomon 2002). Parish (1992) indicated that the katabatic wind regime is responsible for establishment of the polar vortex and that its intensification decays the katabatic drainage. The fact that the katabatic winds are transient events implies that certain mechanism(s)

weaken the horizontal pressure gradient associated with the vortex. Together, this explains why the non-KWE anomaly pattern resembles the SAM.

The anomaly pattern for KWE resembles the third PC (EOF 3), i.e. a wave number 3 pattern with centers of negative height anomalies located in the southern oceans (Figure 5) and positive over most of the Antarctic continent and extending northward in the southeastern Pacific Ocean. On average, the negative anomalies are located to the west (10 to 15°) of the winter mean cyclonic circulation centers of the circumpolar trough (at the surface) and of the 500-hPa troughs. This out of phase pattern for peak-KWE suggests a change in the synoptic-scale activity and/or trajectory of the cyclones around the Antarctic continent. Thus, for example, more cyclonic activity takes place to the northeast of the Ross Sea due to the steering of synoptic-scale cyclones toward the area (Bromwich et al. 1993).

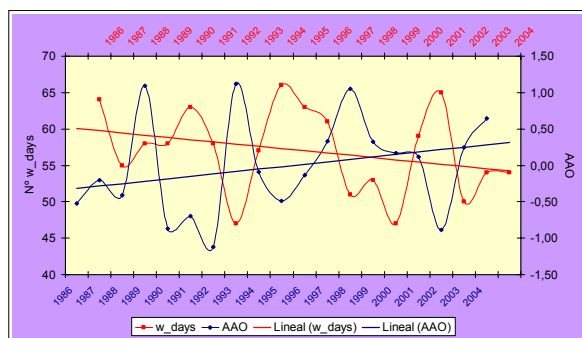


Figure 7. Annual behavior of the katabatic wind days (w_days) and the Antarctic Oscillation Index (AAO, www.cpc.ncep.noaa.gov). Slope of the linear trend of w_days is statistically significant at 10% level, and the correlation between both curves with one year out of phase is statistically significant at 1% level

The synoptic-scale cyclones seen in the KWE anomaly plot act to remove excess vorticity from the polar vortex as they approach the Antarctic continent, and enhance the airflow in the region associated with the katabatic drainage. The removal of vorticity from the polar vortex acts to weaken the overall intensity of vortex. Therefore a negative correlation exists between the number of w_days and the strength of the polar vortex captured by the SAM. The correlation between the w_days and the SAM/AAO index (averaged over April to August) obtained by Marshall (2003) is -0.281 for zero lag, but it increases to -0.481 (statistically significant at 1%

level) for one year lag (Figure 7) with the w_days year preceding the SAM as described above. The correlation improves to -0.58 (statistically significant at 1% level) if it is calculated between the AAO index as obtained by the Climate Prediction Center (www.cdc.ncep.noaa.gov). These lag correlations imply that the time response between the removal (gain) of excess vorticity by the increased (decreased) synoptic-scale activity associated with enhanced (reduced) w_day events, and the subsequent development of a weaker (stronger) polar vortex is approximately one year. Figure 7 also indicates that while SAM/AAO shows a positive trend the w_days shows a negative trend.

The better correlation between w_days (or kw_days) and the CPC-based AAO compared to the Marshall-AAO can be due to the methodologies used to create the indices. The CPC-based AAO index is constructed by projecting the daily and monthly mean 700-hPa height anomalies onto the leading EOF mode using the NCEP/NCAR reanalysis dataset, poleward of 20°S with horizontal resolution of 2.5°×2.5°, while the Marshall (2003) index is constructed based roughly on the difference of sea level pressure observations between 42°S and 70°S. The Marshall (2003) index includes six stations around the coast of the East Antarctic and only three stations at the margin of the southern Pacific Ocean, Puerto Montt, Faraday and Christchurch, and thus the CPC-AAO index might better capture the atmospheric changes occurring in the RIS and the southern Pacific Ocean sectors than the Marshall (2003) index. However further analysis are needed to link the interannual behavior of the katabatic winds and the AAO.

Acknowledgments: This research is part of the Proyecto Anillo, PBCT ACT-19 supported by CONICYT (Comisión Nacional de Investigación de Ciencia y Tecnología).

References

- Bromwich, D.H., 1992: A satellite case study of a katabatic surge along the Transantarctic Mountains. *Int. J. Remote Sensing*, **13**(1), 55-66.
- Bromwich, D.H., J.F. Carrasco and C.R. Stearns, 1992: Satellite observations of katabatic wind propagation for great distances across the Ross Ice Shelf. *Mon. Wea. Rev.*, **120**, 1940-1949.
- Bromwich, D.H., J.F. Carrasco, Z. Liu, and R.-Y. Tzeng, 1993: Hemispheric atmospheric variations and oceanographic impacts associated with katabatic surges across the Ross Ice Shelf. *J. Geophys. Res.*, **98**, 13045-13062.
- Bromwich, D.H., Z. Liu, A.N. Rogers and M.L. Van Woert, 1998: Winter Atmospheric Forcing of the Ross Sea Polynya. In *Ocean, Ice and Atmosphere: Interactions at the Antarctic Continent Margin, Antarctic Research Series*, volume 75, edited by S.S. Jacobs and R. Weiss, 101-133.
- Codron, F., 2005: Relation between Annular Mode and the Mean State: Southern Hemisphere Summer. *J. Climate*, **18**, 320-330.
- Doran, P.T., J.C. Prisco, W.B. Lyons, J.E. Walsh, A.G. Fountain, D.M. McKnight, D.L. Moorhead, R.A. Virginia, D.H. Wall, G.D. Clow, C.H. Fritsen C.P. McKay and A.N. Parsons, 2002: Antarctic climate cooling and terrestrial ecosystem response. *Nature*, **415**, 517-520.
- Jacobs, S.S. and J.C. Comiso, 1989: Sea and ocean process on the Ross Sea continental shelf. *J. Geophys. Res.*, **94**, 18195-18211.
- Marshall, G.J., 2003: Trends in the Southern Annular Mode from observations and reanalyses. *J. Climate*, **14**, 4234-4143.
- Parish, T.R., 1992: On the interaction between Antarctic katabatic winds and tropospheric motions in the high southern latitudes. *Aust. Meteor. Mag.*, **40**, 149-167.
- Parish, T.R., and D.H. Bromwich, 1987: The surface windfield over the Antarctic ice sheets. *Nature*, **328**, 51-54.
- Parish, T.R., and D.H. Bromwich, 1991: Continental-scale simulation of the Antarctic katabatic wind regime. *J. Climate*, **4**(2), 135-146.
- Rosenblüth, B. H. Fuenzalida and P. Aceituno, Recent temperature variations in southern South America. *Int. J. Climatol.*, **17**, 67-85, 1997.
- Thompson, D.W. and S. Solomon, 2002: Interpretation of recent Southern Hemisphere climate change, *Science*, **296**, 895-899.
- Thompson, D.W. and J.M. Wallace, 2000: Annular mode in the extratropical circulation. Part II: Trends. *J. Climate*, **13**, 1000-1016.
- Zwally, H.J., J.C. Comiso, A.L. Gordon, 1985: Antarctic offshore leads and polynyas and oceanographic effects, in *Oceanology of Antarctic Continental Shelf, Antarct. Res. Ser.*, vol. 43, edited by S.S. Jacobs, pp. 203-226, AGU, Washington, D.C.